

## A Mechanical Force Contributes to the “Osmotic Swelling” of Brush-Border Membrane Vesicles

Martin Kirouac,<sup>\*†</sup> Vincent Vachon,<sup>\*†</sup> Mélanie Fortier,<sup>\*†</sup> Marie-Claude Trudel,<sup>\*†</sup> Alfred Berteloot,<sup>\*‡</sup> Jean-Louis Schwartz,<sup>\*‡</sup> and Raynald Laprade<sup>\*†</sup>

<sup>\*</sup>Membrane Protein Research Group; <sup>†</sup>Department of Physics; and <sup>‡</sup>Department of Physiology, University of Montreal, Montreal, Quebec, Canada

**ABSTRACT** Brush-border membrane vesicles and an osmotic swelling assay have been used extensively to monitor the pore-forming activity of *Bacillus thuringiensis* toxins. After a hypertonic shock, *Manduca sexta* midgut brush-border membrane vesicles shrink rapidly and reswell partially to a volume that depends on membrane permeability and toxin concentration rather than regaining their original volume as expected from theoretical models. Because efflux of buffer from the vesicles, as they shrink, could contribute to this phenomenon, vesicles were mixed with a hypertonic solution of the buffer with which they were loaded. Under these conditions, they are not expected to reswell, since the same solute is present on both sides of the membrane. Nevertheless, with several buffers, vesicles reswelled readily, an observation that demonstrates the involvement of an additional restoration force. Reswelling also occurred when, in the absence of toxin, the buffers were replaced by glucose, a solute that diffuses readily across the membrane, but did not occur with rat liver microsomes, despite their permeability to glucose. Unexpected swelling was also observed with rabbit jejunum brush-border membrane vesicles, suggesting that the cytoskeleton, present in brush-border membrane vesicles but absent from microsomes, could be responsible for the restoration force.

### INTRODUCTION

An osmotic swelling assay based on light-scattering measurements is a convenient technique for monitoring continuously the flux of ions or neutral molecules across the membrane of cells or vesicles (1,2). It is usually assumed that, after a hypertonic shock and the resulting initial shrinking, the swelling of the cells or vesicles is due to the entry of water accompanying solute influx driven by the chemical gradient across the membrane (1,2). It has also been suggested that the vesicles could have some restoration forces originating from the elasticity of the membrane and the Donnan effect (1,3), and from the buildup of an internal hydrostatic pressure as the vesicles shrink (4). The light-scattering assay has proven very useful to monitor the pore-forming activity of *Bacillus thuringiensis* insecticidal toxins in lepidopteran midgut brush-border membrane vesicles (2). Once activated by insect midgut proteases, *B. thuringiensis* Cry toxins bind to specific receptors at the surface of midgut epithelial cells and form lethal transmembrane channels (5). The pores formed by these toxins allow the passage of monovalent and divalent anions and cations and relatively large solutes such as sucrose, raffinose, and polyethylene glycols (2,6–11). In receptor-free planar lipid bilayers, the Cry1Ca toxin at high concentrations forms clusters composed of a variable number of similar channels each having a maximal pore radius of 1.0–1.3 nm (12). The osmotic swelling assay

has been used extensively to study the effect of specific mutations (7,10,11,13,14), differential effects of pH (8,15) and ionic strength (15), and the influence of protease inhibitors (16) on the pore-forming properties of the toxins, and to investigate the ionic selectivity of their pores (9).

Despite extensive use of this technique, the kinetics of volume recovery of the vesicles are still not completely understood. After an osmotic shock, in the presence of toxin, vesicles do not reswell to their original volume but reach a constant volume that depends on membrane permeability and toxin concentration. To further characterize the osmotic properties of the vesicles, a series of experiments was performed with *Manduca sexta* midgut brush-border membrane vesicles. Membrane permeability was varied by the addition of the *B. thuringiensis* toxin Cry1Ac or the potassium ionophore valinomycin. The experimental results were compared with those predicted by a mathematical model based on Fick's law of diffusion. Vesicle volume changes due to osmosis are described by Jacobs' equations (1,17,18) for vesicles loaded with an impermeant solute and mixed with both a permeant and an impermeant solute. However, since the pores formed by the toxin are relatively large and non-selective, Jacobs' model was modified to simulate volume changes resulting from the diffusion of two solutes: the buffer with which the vesicles are loaded and the solute used to impose the osmotic shock. Our results demonstrate that, in addition to the chemical gradient across the membrane, a mechanical restoration force contributes to vesicle reswelling. This restoration force is also present in rabbit brush-border membrane vesicles, but not in rat liver microsomes.

Submitted May 9, 2006, and accepted for publication July 18, 2006.

Address reprint requests to Raynald Laprade, Groupe d'étude des protéines membranaires, University of Montreal, PO Box 6128, Centre Ville Station, Montreal, Quebec, H3C 3J7, Canada. Tel.: 514-343-7960; Fax: 514-343-7146; E-mail: raynald.laprade@umontreal.ca.

© 2006 by the Biophysical Society

0006-3495/06/11/3301/12 \$2.00

doi: 10.1529/biophysj.106.088641

## MATERIALS AND METHODS

### Preparation of membrane vesicles

Fertilized *M. sexta* eggs were purchased from the North Carolina State University Entomology Department insectary (Raleigh, NC) and reared on a standard synthetic medium supplied with the insects. Whole midguts were isolated from fifth-instar larvae, freed of attached Malpighian tubules and luminal contents, and rinsed thoroughly with ice-cold 300 mM sucrose, 17 mM Tris-HCl, pH 7.5, and 5 mM EGTA. Brush-border membrane vesicles were prepared with a magnesium precipitation and differential centrifugation technique (19). The final membrane preparation was resuspended in 10 mM Hepes-KOH, pH 7.5, and stored at  $-80^{\circ}\text{C}$  until use.

Rat liver microsomes were prepared with the method of van de Werve (20), with some modifications. Livers from overnight-fasted male Wistar rats (225–250 g) (Charles River, Saint-Constant, Quebec, Canada) were removed, perfused with ice-cold 0.9% (w/v) NaCl and homogenized on ice in 4 ml/g of tissue of 250 mM sucrose, 50 mM Hepes-Tris, pH 7.3, in a Waring blender for 30 s at full speed. The homogenate was then passed 10 times in a Potter homogenizer and centrifuged for 10 min at  $1000 \times g$ . The resulting supernatant was spun at  $12,000 \times g$  for 20 min and the second supernatant was centrifuged at  $100,000 \times g$  for 60 min. The pellet was resuspended in 10 mM Hepes-Tris, pH 7.3, centrifuged at  $100,000 \times g$  for 60 min, resuspended in the same solution, and stored in liquid nitrogen until use.

The proximal small intestines of male New Zealand white rabbits (1.7–2 kg) (Charles River) were removed and flushed with ice-cold 0.9% (w/v) NaCl. Jejunal brush-border membrane vesicles were prepared with a magnesium precipitation and differential centrifugation technique (21,22). The final membrane preparation was resuspended in 10 mM Hepes-Tris, pH 7.3, and stored in liquid nitrogen until use.

### Toxin

The Cry1Ac protoxin was produced from *B. thuringiensis* strain HD73, solubilized, trypsin-activated, and purified by fast protein liquid chromatography, as described earlier (23,24).

### Light-scattering assay

Membrane permeability was analyzed using an osmotic swelling technique based on light-scattering measurements (1,2). In preparation for the experiments, *M. sexta* vesicles were diluted with the appropriate buffer to ~90% of the desired final volume and allowed to equilibrate overnight at  $4^{\circ}\text{C}$ . Before the beginning of the experiments, they were diluted to 0.4 mg of membrane protein/ml and with enough bovine serum albumin to achieve a final concentration of 1 mg/ml. Rabbit vesicles and rat microsomes were diluted directly to 0.4 mg of membrane protein/ml without bovine serum albumin. Rabbit vesicles were allowed to equilibrate overnight at  $4^{\circ}\text{C}$  and microsomes were allowed to equilibrate for at least 60 min at  $4^{\circ}\text{C}$ . In some experiments, for comparison with rabbit vesicles and microsomes, *M. sexta* vesicles were diluted directly to 100% of the desired volume without bovine serum albumin. Vesicles and microsomes were warmed up to  $23^{\circ}\text{C}$  and rapidly mixed with an equal volume of a hypertonic solution using a stopped-flow apparatus (Hi-Tech Scientific, Salisbury, UK). When *M. sexta* vesicles were permeabilized with the *B. thuringiensis* toxin, the vesicles were first incubated with the indicated concentration of toxin for 60 min at  $23^{\circ}\text{C}$  and then submitted to the hypertonic shock. In some experiments, while the vesicles were warming up, the indicated concentrations of valinomycin (Sigma, St. Louis, MO) were added, from a stock solution of 5 mM in ethanol, to both the vesicle suspension and the KSCN solution used for imposing the hypertonic shock. Scattered light intensity was monitored with a photomultiplier tube located at  $90^{\circ}$  from the incident light beam in a Spex Fluorolog CM-3 spectrofluorometer (Jobin Yvon Horiba, Edison, NJ) at a wavelength of 450 nm and a frequency of 10 Hz for most experiments or 400 Hz for the study of the water permeability of the vesicles. In some

experiments, designed to study the influence of the refractive index of the solutions on scattered light intensity, vesicles were replaced by a 0.004% (v/v) suspension of polystyrene latex beads (diameter 105 nm) (Sigma). The refractive index of the solutions was measured with a Reichert AR 200 refractometer (Reichert Analytical Instruments, Depew, NY).

### Data analysis

Scattered light intensity measurements were normalized as follows: the value of 0 was attributed to the intensity measured when the vesicles were diluted with the same solution as that with which they were loaded and the value of 1 was attributed, unless specified otherwise in the figure legends, to the highest intensity measured for a particular set of experiments. Percent volume recovery was defined as  $100(1 - I_t)$ , where  $I_t$  is the relative scattered light intensity measured at a given time  $t$ . Data are mean  $\pm$  SE of the mean of at least three experiments, each performed with a different vesicle preparation. Experimental values for each individual experiment consist of the average of five replicates obtained using the same vesicle preparation. For the study of the water permeability of the vesicles, experimental curves were fitted with the following single exponential function (25) to find the half shrinking time ( $t_{1/2}$ ) of the vesicles:

$$I = I_{\text{Max}}(1 - \exp(-\kappa t)), \quad (1)$$

where  $I$  is the relative scattered light intensity at time  $t$ ,  $I_{\text{Max}}$  is the maximum relative scattered light intensity reached and  $\kappa$  is a rate constant ( $\kappa = \ln(2)/t_{1/2}$ ). Statistical comparisons were made with the two-tailed unpaired Student's  $t$ -test.

### Osmotic swelling simulations

The differential equations developed to describe variations in the volume of the vesicles were solved using a Runge-Kutta algorithm, programmed in Fortran 77 and compiled on a Unix platform. For the purpose of the simulations, vesicles are considered as spheres initially having a diameter of 100 nm, a size that is within the range of those measured for mammalian brush-border membrane vesicles (see, e.g., van Heeswijk and van Os (25)) and a good approximation of those estimated from electron micrographs of lepidopteran midgut brush-border membrane vesicles (see, e.g., Wolfersberger et al. (19)). The water permeability ( $P_w$ ) was set at  $9 \times 10^{-13} \text{ cm}^3/\text{s}$ , a value that allows the vesicles to shrink completely in ~0.2–0.3 s, corresponding to the shrinking time of *M. sexta* brush-border membrane vesicles in our standard osmotic swelling assay used to monitor *B. thuringiensis* toxin activity (8,9). Since the permeabilities to the solutes were adjusted so that the rates of vesicle volume changes corresponded approximately to those observed in the in vitro assay, simulations using somewhat smaller or larger vesicles would yield similar results. For simplicity, the molar volume of the solutes ( $v_A$  and  $v_B$ ) were set equal to that of water ( $v_w$ ) ( $18 \text{ cm}^3/\text{mole}$ ). In these simulations, the volume occupied by the solutes is very small in comparison with that occupied by water. The volume of the vesicles ( $V$ ) was calculated for each value of time and converted to relative volume. In each set of simulations, the value of 0 was attributed to the smallest volume reached and the value of 1 was attributed to the initial volume of the vesicles. Simulations are presented as 1 minus the relative volume to facilitate comparisons with the data derived from light-scattering experiments.

## RESULTS AND DISCUSSION

### Membrane permeability induced by the *B. thuringiensis* toxin Cry1Ac

*M. sexta* midgut brush-border membrane vesicles loaded with 10 mM Hepes-KOH, pH 7.5, were incubated for 60 min with Cry1Ac and submitted to a hypertonic shock by mixing them with an equal volume of the same buffer supplemented with 150 mM KCl or 300 mM sucrose (Fig. 1). Due to the

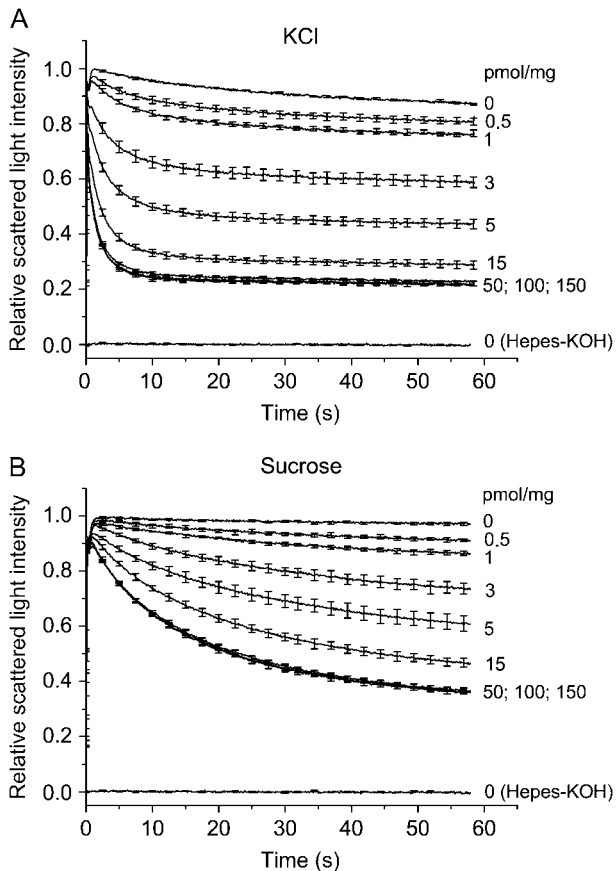


FIGURE 1 Permeability of the pores formed by Cry1Ac to KCl and to sucrose in *M. sexta* midgut brush-border membrane vesicles. *M. sexta* brush-border membrane vesicles equilibrated overnight in 10 mM Hepes-KOH, pH 7.5, were incubated for 60 min with the indicated concentrations of Cry1Ac (in pmol toxin/mg membrane protein). They were then mixed with an equal volume of the same solution as that with which they were loaded (Hepes-KOH) or with 10 mM Hepes-KOH, pH 7.5, and (A) 150 mM KCl or (B) 300 mM sucrose. All solutions contained 1 mg/ml bovine serum albumin. For clarity, error bars are shown for every 25th experimental point.

osmotic shock, water exited from the vesicles and their volume decreased rapidly, as evidenced by a sharp rise in scattered light intensity. Then, vesicles reswelled and subsequently recovered some of their original volume. As was observed in previous studies on *B. thuringiensis* toxins (2,7–11,15,16), vesicles reswelled partially to a volume that depended on membrane permeability rather than regaining their original volume. The rate and magnitude of vesicle swelling, which depend on the permeability of the membrane to the solute, increased, as expected, with toxin concentration. Vesicles reswelled faster with KCl than with sucrose, in agreement with previous studies (2,8).

### Relation between vesicle volume and scattered light intensity

*M. sexta* vesicles loaded with 1, 10, or 100 mM Hepes-KOH, pH 7.5, were rapidly mixed with an equal volume of solu-

tions containing various concentrations of KCl (Fig. 2). The volume of the vesicles decreased as indicated by a rise in scattered light intensity when the ratio between the osmolarities inside and outside the vesicles was  $<1$ . In the standard assay used to test the activity of *B. thuringiensis* toxins (Fig. 1), the initial ratio between the osmolarities inside and outside the vesicles is  $\sim 0.09$ . Therefore, in Fig. 2, to facilitate comparisons with the results obtained with the standard assay, scattered light intensities were normalized with those measured for this ratio. Since the relation between scattered light intensity and the ratio between the osmolarity inside and outside the vesicles was not always linear, the vesicles did not appear to shrink as expected for ideal osmometers and predicted by the Boyle-Van't Hoff relation (26). The relation tended to become somewhat more linear when the osmolarity of the buffer solution with which the vesicles were loaded was increased from 1.5 (Fig. 2 A) to 15 mOsm/l (Fig. 2 B), as in the standard assay, or 150 mOsm/l (Fig. 2 C). In the experiments illustrated in Fig. 2, A and B, the vesicle volume never seemed to reach a minimum even for the smallest ratios tested.

Variations in scattered light intensity are influenced by the refractive index of the surrounding medium (27,28). To test how the variation in refractive index of the KCl solutions influenced the scattered light intensity measurements shown in Fig. 2, the vesicles were replaced by a suspension of nonosmotically sensitive polystyrene latex beads. Since salt-induced aggregation of latex beads has been reported (29), the KCl solutions were replaced by solutions of sucrose having the same refractive index. No significant change in scattered light intensity attributable to changes in the refractive index of the solutions was observed under the conditions used for the experiment illustrated in Fig. 2 A. Changes in the refractive index accounted for  $0.09 \pm 0.01$  and  $0.17 \pm 0.03$  relative scattered light intensity units, between the smallest and highest osmolarity ratios, in Fig. 2, B and C, respectively, and for  $<0.05$  units between the osmolarity ratios of 0.09 and 1, in both experiments. Even if changes in refractive index slightly influenced the scattered light intensities, these changes were too small, in comparison with those due to changes in volume, to explain the shape of the curves presented in Fig. 2 or the differences observed between the curves depicted in Fig. 2, A–C.

A possible nonlinear relation between the volume of the vesicles and scattered light intensity, potential structural limitations of the membrane, or a nonnegligible permeability of the membrane to KCl and to Hepes-KOH could possibly contribute to the fact that, in Fig. 2, the volume of the vesicles does not appear to vary as expected for an ideal osmometer. A nonlinear relation between scattered light intensity and imposed osmotic gradient has already been reported for *M. sexta* midgut vesicles loaded with 10 mM Ches-KOH and submitted to various hypertonic solutions of KCl (6). However, this result contrasts with those of other studies that report a quasilinear relation for hog gastric

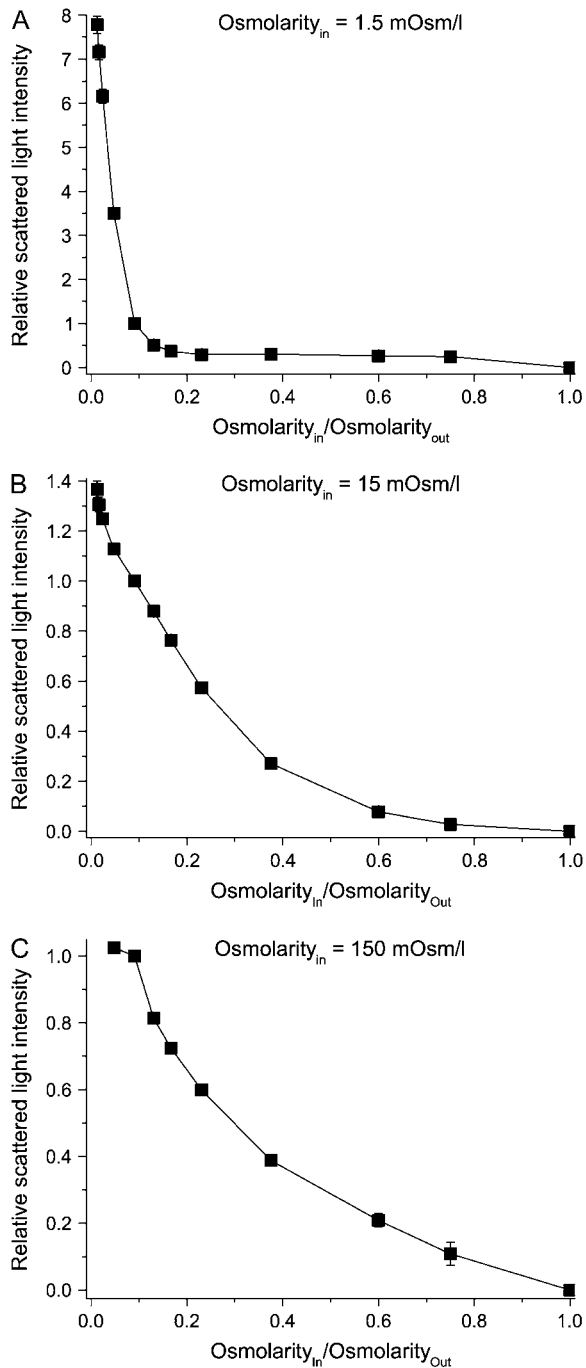


FIGURE 2 Relation between scattered light intensity and volume of *M. sexta* vesicles. Vesicles incubated overnight in (A) 1, (B) 10, or (C) 100 mM HEPES-KOH, pH 7.5, were submitted to a hypertonic shock by mixing them rapidly with an equal volume of a solution containing the buffer with which they were loaded and enough KCl to reach the indicated osmolarity ratios. All solutions contained 1 mg/ml bovine serum albumin. The maximum scattered light intensity measured for each ratio was converted into relative scattered light intensity. The value of 0 was attributed to the intensity measured when the vesicles were diluted with the same solution as that with which they were loaded and the value of 1 was attributed to that reached when the osmolarity ratio was equal to 0.09.

vesicles (30), rabbit renal brush-border membrane vesicles (31), and rabbit renal basolateral membrane vesicles (32). Worman and Field (33) reported a deviation from linearity when rat small intestine brush-border membrane vesicles were submitted to large osmotic gradients. In these studies, vesicles were loaded with solutions having an osmolarity comparable (102 mOsm/l) (33) or superior (from 265 to 320 mOsm/l) (30–32) to that of the solutions used to load the vesicles in the experiments illustrated in Fig. 2. They were also submitted to a smaller range of osmolarity ratios, thus avoiding the region where the ratio between the osmolarity inside and outside the vesicles is  $<0.2$ , in which the curve shown in Fig. 2 C deviates most from linearity. A quasilinear relation was also observed for rabbit skeletal muscle sarcoplasmic reticulum vesicles over a range of osmolarity ratios similar to that shown in Fig. 2 C (34), but these experiments are difficult to compare with those illustrated in Fig. 2, since, in contrast to our experimental design, the osmolarity inside the vesicles was varied and the osmolarity outside the vesicles was kept constant.

In the standard assay (Fig. 1), the relative scattered light intensity varies between 1, at the apex of the control curves recorded without toxin, and 0.2–0.4, 60 s after the osmotic shock at saturating toxin concentrations. Within this range, the calibration curve is reasonably linear (Fig. 2 B). At saturating toxin concentrations, scattered light intensities never returned to the value measured in the absence of an osmotic shock. According to experiments performed with latex beads, this cannot be due to changes in the refractive index between the HEPES-KOH and the KCl solutions. Furthermore, this cannot be explained by a direct effect of the toxin on scattered light intensity since no change in this parameter was observed in the absence of an osmotic shock when vesicles incubated with toxin were mixed with the solution with which they were loaded (2). The observation that the vesicles never appear to regain their initial volume may suggest that the vesicle preparations could be contaminated with membranes other than the brush-border membrane, such as the basolateral membrane, in which the toxin is unable to form pores (35,36). To test this hypothesis, experiments similar to those illustrated in Fig. 1 were performed with vesicles loaded with HEPES-KOH and exposed to a hypertonic solution of KSCN in the presence of various concentrations of valinomycin (Fig. 3). Vesicles reswelled at a rate that depended on valinomycin concentration. At low valinomycin concentrations, the rate of vesicle swelling is limited by the valinomycin-induced membrane permeability to potassium ions, whereas at high concentrations, the rate of vesicle swelling is limited by the finite membrane permeability to thiocyanate ions. Results obtained with valinomycin (Fig. 3) are similar to those obtained with the toxin (Fig. 1) and, even at high valinomycin concentrations, vesicles never regained their initial volume. This had already been observed with *M. sexta* vesicles (2) and with rabbit sarcoplasmic reticulum vesicles (34). Thus, the presence of other membranes

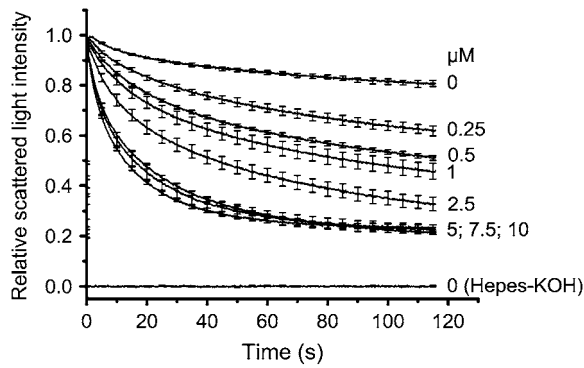


FIGURE 3 Permeability of *M. sexta* vesicles to KSCN in the presence of various concentrations of valinomycin. Vesicles equilibrated in 10 mM HEPES-KOH, pH 7.5, were mixed with an equal volume of the same solution as that with which they were loaded (HEPES-KOH) or with 150 mM KSCN and 10 mM HEPES-KOH, pH 7.5. The indicated concentration of valinomycin was added to both the vesicle suspension and the solution used to impose the hypertonic shock. All solutions contained 1 mg/ml bovine serum albumin. For clarity, error bars are shown for every 50th experimental point.

cannot explain why, in Fig. 1, scattered light intensities never returned to their initial values even at saturating toxin concentrations.

### Simulation of volume changes

A model based on Fick's law of diffusion, similar to that proposed by Jacobs (17), was developed to analyze the theoretical effect of various factors on vesicle swelling. To simulate changes in the volume of vesicles having a permeability not only to one but to two solutes, a third differential equation was added to those of Jacobs (17). The theoretical vesicles contain  $X_A$  moles of solute A,  $X_B$  moles of solute B, and  $X_W$  moles of water and have the permeabilities across the membrane (in  $\text{cm}^3/\text{s}$ )  $P_A$ ,  $P_B$ , and  $P_W$  for solutes A and B and water, respectively. At time 0, the vesicles are mixed with A and B at the osmolarities  $C_A$  and  $C_B$ . It is assumed that both osmolarities do not change over time. The following equations describe the variation in the number of moles of A, B, and water inside the vesicles over time  $t$ :

$$\frac{dX_A}{dt} = P_A \left( C_A - \frac{X_A}{V} \right) \quad (2)$$

$$\frac{dX_B}{dt} = P_B \left( C_B - \frac{X_B}{V} \right) \quad (3)$$

$$\frac{dX_W}{dt} = P_W \left[ \frac{X_A + X_B}{V} - (C_A + C_B) \right]. \quad (4)$$

The volume  $V$  of the vesicles can be calculated for each value of  $t$  with the following equation:

$$V(t) = v_A X_A(t) + v_B X_B(t) + v_W X_W(t), \quad (5)$$

where  $v_A$ ,  $v_B$ , and  $v_W$  are the molar volumes of A, B, and water, respectively. In Jacobs' equations, the permeabilities are given in  $\text{cm}/\text{s}$  and multiplied by the area of the membrane. In our model, it is assumed that the area of the membrane does not change over time and the permeabilities are expressed directly in  $\text{cm}^3/\text{s}$ . Jacobs' equations were modified earlier by Johnson and Wilson (37) to include Staverman's reflection coefficient, which is based on irreversible thermodynamics (18,38). This coefficient must be taken into account when experimental data are fitted with a theoretical model to determine the permeabilities of the membrane. However, since only qualitative comparisons between the experimental data and simulated experiments are presented in this study, the reflection coefficient was neglected. Equations 2–4 were solved for various permeabilities  $P_A$  and  $P_B$ , as described under Materials and Methods (Fig. 4). According to the simulations, if the membrane is only permeable to the solute used to impose the osmotic shock, the vesicles should reswell to their initial volume at a rate that depends on the permeability of the membrane for this solute (Fig. 4 A). On the other hand, if the membrane is also

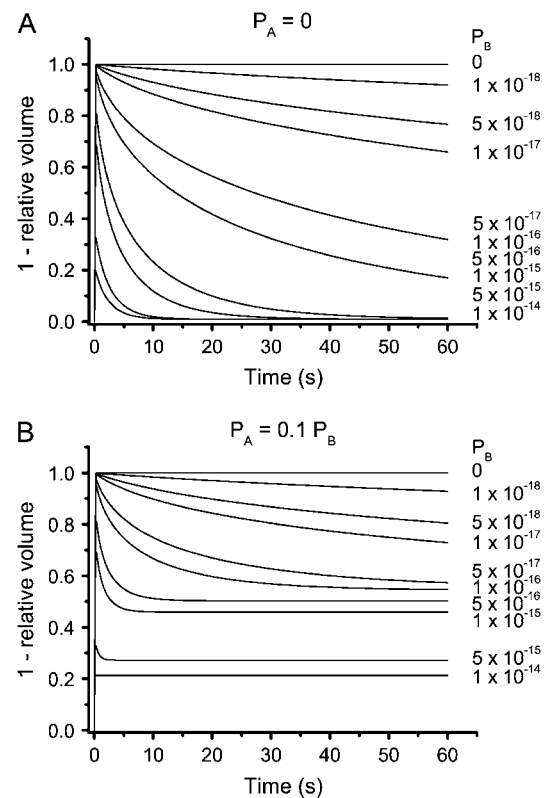


FIGURE 4 Variations in the volume of the vesicles predicted by the mathematical model. The simulated vesicles are spheres having a diameter of 100 nm and containing 15 mOsm/l of solute A dissolved in water. At time 0, the vesicles are mixed instantaneously with a solution containing 15 mOsm/l of solute A and 150 mOsm/l of solute B. Membrane permeabilities to the different solutes were: (A) 0 or (B)  $0.1 \times P_B$  for solute A and the indicated permeabilities ( $P_B$ ) for solute B (in  $\text{cm}^3/\text{s}$ ).

permeable to the buffer with which the vesicles are loaded, they are predicted to regain only a fraction of their original volume depending on membrane permeability (Fig. 4 B). Efflux of buffer during the shrinking phase of the experiment could therefore tentatively explain why, in the osmotic swelling assay, the vesicles reswelled only partially, even at saturating toxin concentrations (Fig. 1).

In this model,  $P_W$  was kept constant when the permeability to the solute was varied. However, since the pores formed by the toxin allow the diffusion of relatively large solutes, they are also expected to be permeable to water. Previous studies have reported an effect of Cry toxins on water permeability based on experiments in which the rate of vesicle shrinkage after an osmotic shock of KCl (39,40) or sucrose (2) increased as a function of toxin concentration. To test whether it was appropriate to use a constant  $P_W$  in the simulations, we first searched for a salt that is unable to diffuse through the pores formed by the toxin. An impermeable solute can be found based on the cationic selectivity of the pores (9,41–46) and the fact that osmotic swelling caused by a dissociated salt depends on the influx of both ion species and is limited by the rate of diffusion of the least permeable ion (2,8). Indeed, in agreement with the anion being the rate limiting species, amino acids bearing a net negative charge diffuse more slowly through the pores formed by *B. thuringiensis* toxins than neutral or positively charged amino acids (9). Also, slower diffusion rates were observed for the potassium salts of divalent anions than for the chloride salts of divalent cations (9). Consequently, at pH 7.5, the permeability to a solute composed of a trivalent anion, such as Tris-citrate, is expected to be very low. This hypothesis was confirmed with experiments performed with *M. sexta* vesicles loaded with 10 mM HEPES-KOH, pH 7.5, incubated for 60 min with various concentrations of Cry1Ac and mixed with a solution composed of 150 mM Tris-citrate and 10 mM HEPES-KOH, pH 7.5 (Fig. 5 A). In the absence of toxin, the membrane has a small permeability to Tris-citrate. Increasing toxin concentration caused the vesicles to shrink to a smaller volume rather than increasing the rate at and extent to which they reswelled. This observation probably results from the inability of Tris-citrate to diffuse across the pores formed by the toxin and from a nonnegligible permeability of these pores to HEPES-KOH that overcomes the endogenous permeability of the membrane to Tris-citrate. Thus, HEPES-KOH could leak out of the vesicles in response to its increased concentration after vesicle shrinking. Such a permeability to HEPES-KOH is not apparent in Fig. 1, probably because the pores are more permeable to KCl and sucrose than to HEPES-KOH.

To test the water permeability of the pores, vesicles were therefore loaded with 10 mM Tris-citrate, pH 7.5, incubated with various concentrations of Cry1Ac, and submitted to a hypertonic solution of 150 mM Tris-citrate (Fig. 5 B). The curves were then fitted with Eq. 1. The half shrinking times ( $t_{1/2}$ ) of the vesicles calculated in the presence of 0, 5, 15, 50, 100, and 150 pmol of toxin/mg membrane protein were

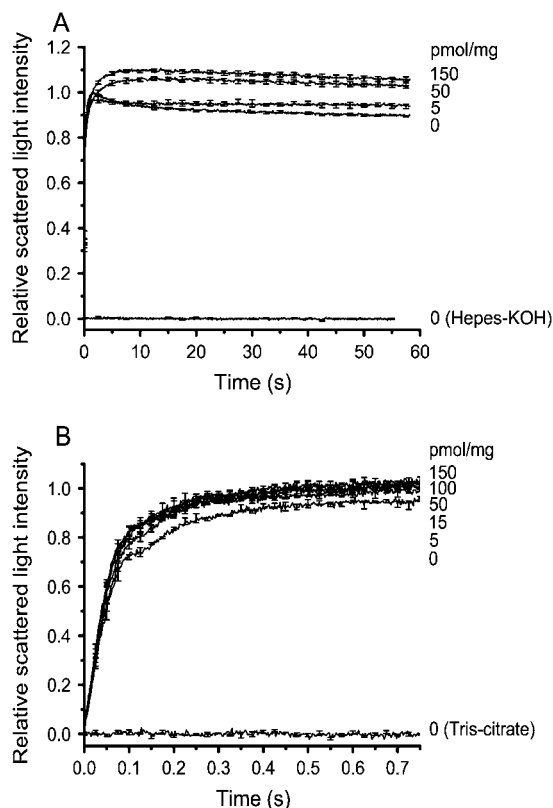


FIGURE 5 Permeability of the pores formed by Cry1Ac to Tris-citrate and to water. *M. sexta* vesicles equilibrated overnight in (A) 10 mM HEPES-KOH or (B) 10 mM Tris-citrate, pH 7.5, were incubated for 60 min with the indicated concentrations of Cry1Ac (in pmol toxin/mg membrane protein). They were then mixed with an equal volume of the same solution as that with which they were loaded (HEPES-KOH or Tris-citrate), or with (A) 150 mM Tris-citrate and 10 mM HEPES-KOH, pH 7.5, or (B) 150 mM Tris-citrate, pH 7.5. The value 0 was attributed to the scattered light intensity measured when the vesicles were diluted with the same solution as that with which they were loaded and the value 1 was attributed (A) to the maximum intensity reached without toxin or (B) to the mean intensity reached between 0.5 and 1 s. For clarity, error bars are shown for every (A) 25th or (B) 10th experimental point.

equal to  $49 \pm 2$ ,  $46 \pm 1$ ,  $45 \pm 3$ ,  $41 \pm 1$ ,  $41 \pm 2$ , and  $40 \pm 2 \times 10^{-3}$  s, respectively. Only  $t_{1/2}$  values calculated for 50, 100, and 150 pmol of toxin/mg membrane protein were significantly different ( $p < 0.05$ ) from the value obtained without toxin. The rates of vesicle shrinking induced by Tris-citrate and calculated from the initial slopes of the curves shown in Fig. 5 B were not significantly different from each other ( $p > 0.05$ ). Since the toxin did not change substantially the already large water permeability of the membrane, it appears justified to use a constant water permeability, as a reasonable approximation, in the simulations presented in Fig. 4.

#### Effect of the buffer permeability of the pores formed by Cry1Ac on vesicle swelling

Since valinomycin is very selective for potassium ions, no efflux of buffer is expected through this ionophore. In

contrast with the prediction of the model (Fig. 4 A), the results obtained with valinomycin (Fig. 3) were similar to those obtained with the toxin (Fig. 1). As another means of testing the hypothesis that efflux of buffer during the shrinking phase of the experiment could explain why the vesicles reswelled to a volume that depended on toxin concentration, experiments similar to those illustrated in Fig. 1 were performed with vesicles loaded with 10 mM Tris-citrate, pH 7.5, and mixed with 150 mM KCl and 10 mM Tris-citrate, pH 7.5 (Fig. 6). To summarize a large number of similar experiments and to facilitate their comparison, data are presented as percent volume recovery values measured after 30 s. Replacing Hepes-KOH by Tris-citrate did not change significantly the rate and extent of vesicle swelling in the presence of KCl. Therefore, efflux of buffer during the shrinking phase of the experiment cannot explain why the vesicles reswell only partially since this is also observed when buffer efflux is prevented by replacing the toxin by valinomycin and in the presence of an impermeable buffer, Tris-citrate. A possible explanation may be that the large extent of shrinking may alter the mechanical integrity of the vesicles and prevent them from completely resuming their original volume over the time course of the experiments.

### Reswelling in the presence of the same solute inside and outside the vesicles

Vesicles are not expected to reswell when they are mixed with a hypertonic solution of the buffer with which they are loaded since they should only shrink until the buffer concentration becomes equal on both sides of the membrane. Because solute influx can occur as the vesicles shrink, however, the model predicts that the vesicles will only shrink to a volume that depends on the permeability of the membrane to the solute (Fig. 7 A). However, when incubated with Cry1Ac, vesicles loaded with 10 mM Hepes-KOH, pH 7.5,

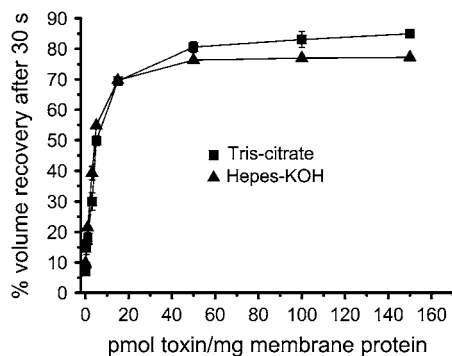


FIGURE 6 Effect of buffer composition on apparent membrane permeability to KCl. *M. sexta* vesicles were loaded with 10 mM Tris-citrate (■) or Hepes-KOH (▲), pH 7.5, and incubated for 60 min with the indicated concentrations of Cry1Ac. Vesicles were mixed with an equal volume of a solution containing 150 mM KCl and the buffer with which they were loaded. All solutions contained 1 mg/ml bovine serum albumin.

reswelled readily after having been mixed with 150 mM Hepes-KOH, pH 7.5 (Fig. 7 B). This result suggests the involvement of an additional restoration force that allows the vesicles to reswell when they are mixed with a hypertonic solution of the buffer with which they are loaded. Furthermore, in contrast with the simulations (Fig. 7 A), even at saturating toxin concentrations, the actual vesicles shrank to a volume close to that attained in the absence of toxin (Fig. 7 B). This indicates that the toxin can only permeabilize the membrane to a certain extent that is probably limited by the number of toxin receptors present at the surface of the membrane. To model vesicle reswelling under these conditions, a term describing a hypothetical “mechanical force” can be added to Eq. 4, which becomes

$$\frac{dX_w}{dt} = P_w \left[ \frac{X_A + X_B}{V} - (C_A + C_B) \right] - P_w k C_w \left( 1 - \frac{V_0}{V} \right), \quad (6)$$

where  $C_w$  is the concentration of water,  $V_0$  is the initial volume of the vesicles, and  $k$  is a return constant. The mechanical term is equal to zero, before shrinking, when the volume of the vesicles is equal to their initial volume, and opposes shrinking increasingly as the volume of the vesicles decreases. When Eq. 4 is replaced by Eq. 6, the model predicts that the vesicles should reswell even when they are mixed with a hypertonic solution of the buffer with which they are loaded (Fig. 7 C). In agreement with this prediction, vesicles loaded with 10 mM KCl and 0.1 mM Hepes-KOH, 20 mM sucrose and 0.1 mM Hepes-KOH, 10 mM imidazole-HCl, 10 mM Tris-HCl, or 10 mM Caps-KOH and mixed with a hypertonic solution of the same compounds reswelled readily (Fig. 7 D). In contrast, volume recoveries of only ~5% were observed with Tris-citrate in the presence and absence of toxin (Fig. 7 D), in agreement with the small permeability of the membrane for this solute, which cannot be increased by the addition of toxin (Fig. 5 A). In these experiments, the pH of the imidazole-HCl, Tris-HCl, Hepes-KOH, and Caps-KOH solutions were adjusted to the pKa of the organic species to ensure the presence of an equal ratio between the charged and uncharged species of each buffer. A small concentration of Hepes-KOH was kept in the solutions of KCl and sucrose used to load the vesicles to maintain a constant pH. In agreement with a cationic selectivity of the pores, similar percent volume recoveries were observed with imidazole-HCl, Tris-HCl, and KCl, irrespective of the size of the cation. Lower percent volume recovery values were recorded for Caps-KOH and Hepes-KOH, although similar levels were reached for both buffers, which are composed of a larger anion. In the presence of an osmotic shock of KCl, vesicle swelling was remarkably similar for vesicles loaded with 10 mM Hepes-KOH or with 10 mM KCl and 0.1 mM Hepes-KOH (Fig. 7 E). In the presence of sucrose, vesicle swelling was only slightly lower when the vesicles were loaded with 20 mM sucrose and 0.1 mM Hepes-KOH

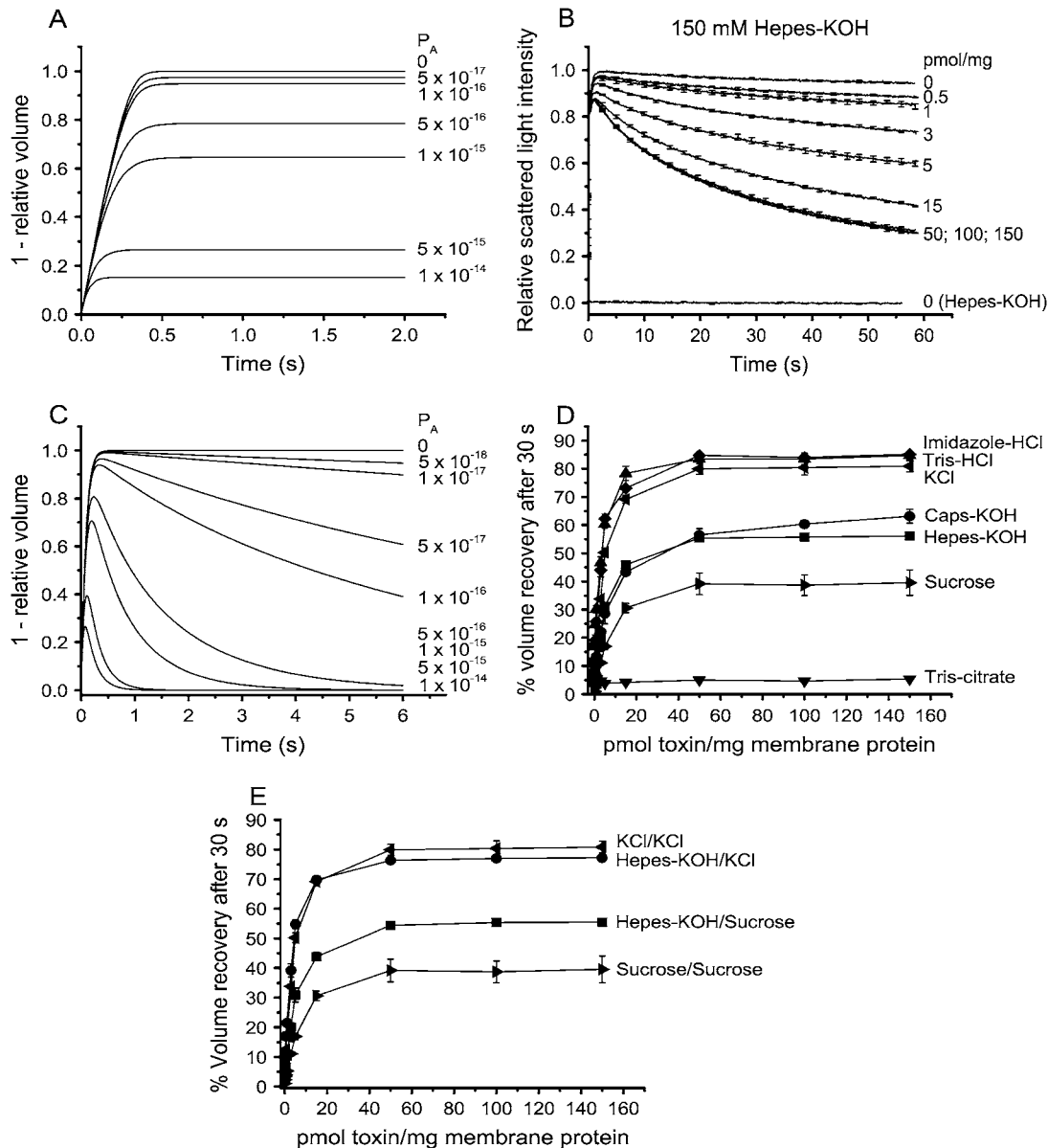


FIGURE 7 Changes in the volume of vesicles exposed to the same solute on both sides of the membrane. (A) Predicted volume of vesicles loaded with 15 mOsm/l of solute A and mixed with 150 mOsm/l of the same solute. The membrane has the indicated permeabilities ( $P_A$ ) to the solute (in  $\text{cm}^3/\text{s}$ ). In these simulations, no solute B is present. (B) *M. sexta* vesicles loaded with 10 mM Hepes-KOH, pH 7.5, and incubated for 60 min with the indicated concentrations of Cry1Ac (in pmol toxin/mg membrane protein) were mixed with an equal volume of the same solution as that with which they were loaded (Hepes-KOH) or with 150 mM Hepes-KOH, pH 7.5. For clarity, error bars are shown for every 25th experimental point. (C) Modeling of vesicle volume was performed as in A except that Eq. 4 was replaced by Eq. 6 to take into account a mechanical force with  $k = 2 \times 10^{-4}$ . (D) The experiments were similar to those presented in panel B; Hepes-KOH, pH 7.5 (■), was replaced in both the solutions used for loading the vesicles and those used for the osmotic shock by the same concentrations of imidazole-HCl, pH 6.95 (◆), Tris-HCl, pH 8.1 (▲), Tris-citrate, pH 7.5 (▼), Caps-KOH, pH 10.5 (●), KCl (◄), or isotonic solutions of sucrose (►). Solutions containing KCl and sucrose also contained 0.1 mM Hepes-KOH, pH 7.5. (E) Vesicles loaded with 10 mM Hepes-KOH, pH 7.5, and incubated for 60 min with the indicated concentrations of Cry1Ac were mixed with an equal volume of a solution containing 150 mM KCl (●, *Hepes-KOH/KCl*) or 300 mM sucrose (■, *Hepes-KOH/Sucrose*) and 10 mM Hepes-KOH, pH 7.5. Vesicles loaded with KCl were submitted to a hypertonic solution of KCl (◄, *KCl/KCl*) and vesicles loaded with sucrose were submitted to a hypertonic solution of sucrose (►, *Sucrose/Sucrose*). All solutions contained 1 mg/ml bovine serum albumin.

than when they were loaded with 10 mM Hepes-KOH (Fig. 7 E). Taken together, these results strongly suggest that in the standard osmotic swelling assay, a mechanical force contributes substantially to the osmotic swelling of the

vesicles. They also stress that whatever the driving force, the rate and extent of vesicle swelling after the initial shrinking is controlled by the membrane permeability to the solute.



As a corollary, the mechanical force added in Eq. 6 that promotes vesicle reswelling also imposes a constraint on vesicle shrinking and may explain why, in the absence of toxin, the vesicles do not appear to shrink as expected from ideal osmometers in Fig. 2. When  $k \neq 0$  and the simulated vesicles loaded with 1.5, 15, or 150 mM of solute A are mixed with hypertonic solutions of solute A (or with a mixture of solutes A and B), Eq. 6 predicts nonlinear relationships between the minimum volume of the vesicles (when  $dX_w/dt = 0$ ) and the ratio between the intravesicular and extravesicular osmolarities (Fig. 8) which follow a pattern remarkably similar to that measured experimentally (Fig. 2). Like Fig. 2, Fig. 8 shows that for the same osmolarity ratios, the curves become increasingly linear as the intravesicular osmolarity is increased (Fig. 8, A–C). Thus, the same hypothetical mechanical force can explain not only why the vesicles reswelled in the presence of toxin when the osmotic shock was imposed with the same solute as that with which the vesicles were loaded, but also why they did not shrink as expected from ideal osmometers.

### Origin of the restoration force

Experiments that highlight the additional restoration force can also be performed without prior membrane permeabilization with toxin or valinomycin. *M. sexta* vesicles loaded with 10 mM HEPES-Tris, pH 7.3, were mixed with an equal volume of the same buffer supplemented with 400 mM sucrose or glucose (Fig. 9 A). In agreement with previous work (2), glucose diffused readily across the midgut membrane of *M. sexta*, whereas sucrose was impermeant. Reswelling was also observed when *M. sexta* vesicles were loaded with 20 mM glucose and 1 mM HEPES-Tris, and submitted to a hypertonic shock of glucose (Fig. 9 B). Similar experiments were conducted with rat liver microsomes (Fig. 9, C and D), also known to be more permeable to glucose than to sucrose (47). In contrast with *M. sexta* vesicles, and despite their larger permeability to glucose than to sucrose (Fig. 9 C), microsomes loaded with glucose and mixed with a hypertonic solution of glucose reswelled at the same rate as those mixed with sucrose (Fig. 9 D). These results clearly show that the mechanical restoration force is much weaker in the microsomes than in the vesicles.

To test whether a restoration force is also present in other types of brush-border membrane vesicles, experiments were carried out to compare vesicles prepared from rabbit jejunum and from *M. sexta* midguts. Insect vesicles, loaded with 10 mM HEPES-Tris, pH 7.3, were first mixed with the same buffer supplemented with 150 mM KSCN (Fig. 10 A). Vesicles have a nonnegligible endogenous permeability to KSCN that can be increased with the addition of valinomycin. *M. sexta* vesicles, also reswelled readily when they were loaded with 10 mM KSCN and 1 mM HEPES-Tris and mixed with a hypertonic solution of KSCN (Fig. 10 B). Rabbit brush-border membrane vesicles also reswelled readily after

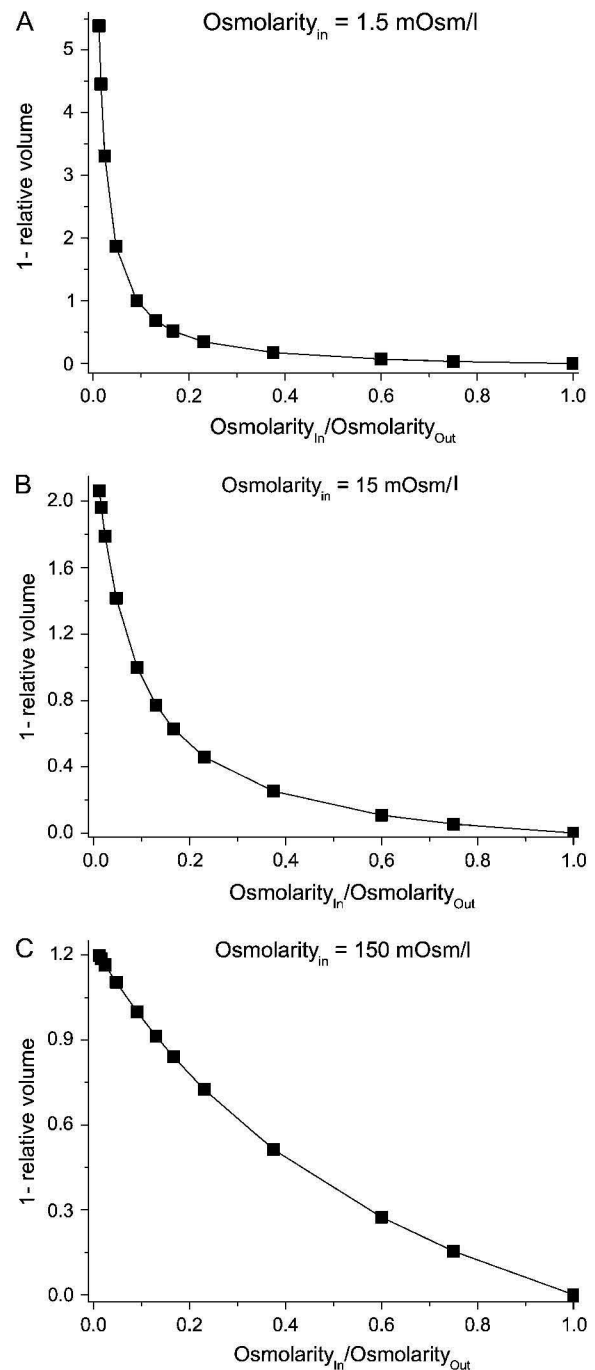


FIGURE 8 Theoretical relation between the volume of the vesicles and the ratio of the osmolarities inside and outside of the vesicles in the presence of a mechanical force and in the absence of toxin. The simulated vesicles contain (A) 1.5, (B) 15, or (C) 150 mM of solute A dissolved in water. The vesicles are mixed instantaneously with a solution containing enough solute A to reach the indicated osmolarity ratios. The minimum volume of the vesicles reached after equilibrium, when  $dX_w/dt = 0$ , was calculated with Eq. 6 with the return constant  $k = 2 \times 10^{-4}$ .

having been exposed to a hypertonic solution of KSCN whether they were loaded with KSCN (Fig. 10 D) or not (Fig. 10 C). These results suggest that the cytoskeleton, present in brush-border membrane vesicles but absent

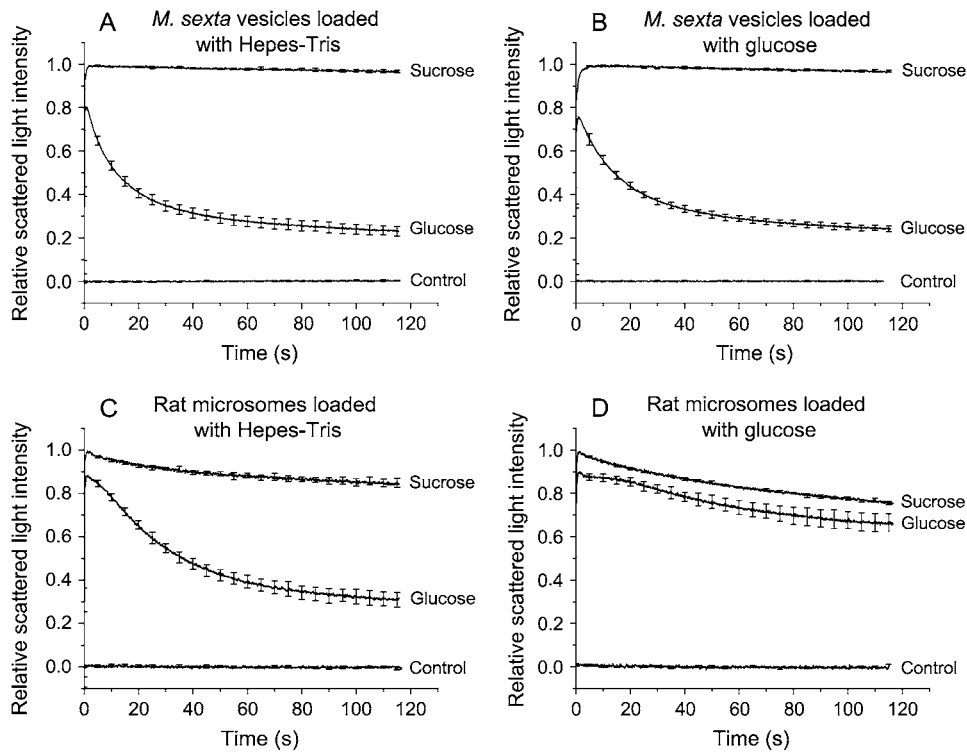


FIGURE 9 Comparison of the osmotic swelling of *M. sexta* brush-border membrane vesicles and rat liver microsomes. (A and B) *M. sexta* vesicles or (C and D) rat microsomes were loaded with (A and C) 10 mM Hepes-Tris, pH 7.3, or with (B and D) 20 mM glucose and 1 mM Hepes-Tris, pH 7.3, and mixed with an equal volume of (A and C) 400 mM sucrose and 10 mM Hepes-Tris, pH 7.3 (Sucrose), or 400 mM glucose and 10 mM Hepes-Tris, pH 7.3 (Glucose), (B and D) 400 mM sucrose, 20 mM glucose, and 1 mM Hepes-Tris, pH 7.3 (Sucrose), or 420 mM glucose and 1 mM Hepes-Tris, pH 7.3 (Glucose), or with the solution with which they were loaded (Control). For clarity, error bars are shown for every 50th experimental point.

from microsomes, could be responsible for the restoration force.

The existence of a mechanical force does not question the interpretation of results presented in previous studies on *B. thuringiensis* toxins, in which the osmotic swelling assay

was used to monitor toxin pore formation, since vesicle swelling only occurs when the membrane is permeable to the external solute. Furthermore, in these studies only qualitative comparisons were made between the swelling rates induced by the toxins. However, calculations of the permeability of

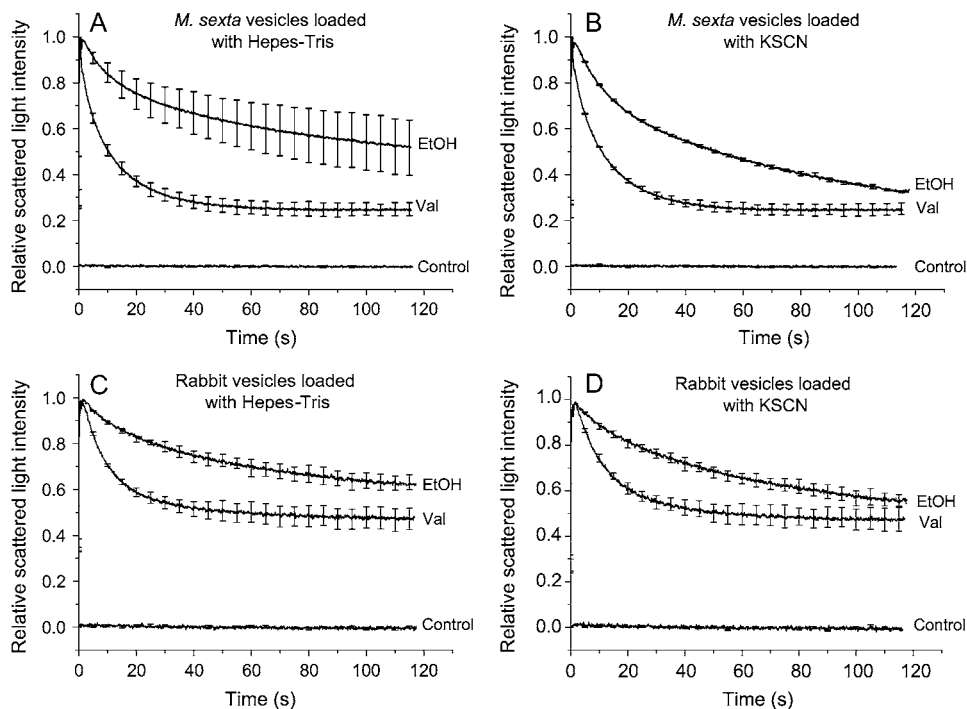


FIGURE 10 Osmotic swelling of *M. sexta* and rabbit intestinal brush-border membrane vesicles. (A and B) *M. sexta* or (C and D) rabbit brush-border membrane vesicles were loaded with (A and C) 10 mM Hepes-Tris, pH 7.3, or (B and D) 10 mM KSCN and 1 mM Hepes-Tris, pH 7.3, and mixed with an equal volume of (A and C) 150 mM KSCN and 10 mM Hepes-Tris, pH 7.3, (B and D) 160 mM KSCN and 1 mM Hepes-Tris, pH 7.3, or the solution with which they were loaded (Control). The vesicle suspensions and solutions contained 7.5  $\mu$ M valinomycin (Val) or an equivalent concentration of ethanol (EtOH). For clarity, error bars are shown for every 50th experimental point.

the membrane to a solute from the results obtained with brush-border membrane vesicles and an osmotic swelling assay should take into account the possible contribution of an additional mechanical force. The intrinsic mechanical and elastic properties of the membrane of liposomes and vesicles have been studied in detail (4,48–52), but such forces could not explain our results since they are also expected to be present in microsomes and in brush-border membrane vesicles. Reswelling when the solute inside and outside the vesicles is the same has also been reported earlier. Kidney brush-border membrane vesicles loaded with mannitol and submitted to a hypertonic shock of mannitol reswelled, but no reswelling was observed when mannitol was replaced by cellobiose (4). These results were interpreted as indicating that kidney vesicles have a small membrane permeability to mannitol but are impermeable to cellobiose. In contrast with our experiments, reswelling took as long as 10 h. It was proposed that after the osmotic shock and subsequent vesicle shrinking there remains a chemical gradient of mannitol, probably due to a hydrostatic pressure caused by the presence of osmotically active molecules inside the vesicles. This hydrostatic pressure could play a role similar to that of our mechanical force added in Eq. 6, since it can also explain why kidney vesicles do not behave like perfect osmometers (4). However, in our experiments, the amplitude of such a hydrostatic force should be rather small, since osmotically active molecules present inside the vesicles are expected to diffuse through the pores formed by the toxin during the 60-min incubation of the vesicles before the osmotic shock and during the vesicle shrinking phase of the experiments.

## CONCLUSION

The above results strongly suggest that a mechanical force contributes to the reswelling of brush-border membrane vesicles after a hypertonic shock. This force could also explain why brush-border membrane vesicles do not appear to shrink as expected for ideal osmometers. The fact that the mechanical force is much less evident in rat liver microsomes than in brush-border membrane vesicles suggests that the cytoskeleton could be at its origin. Our results also clearly demonstrate that efflux of buffer during the shrinking phase of the osmotic swelling assay does not appear to be sufficient to explain why *M. sexta* brush-border membrane vesicles reswell partially to a volume that depends on membrane permeability induced by *B. thuringiensis* toxins or by valinomycin since it occurs in the presence of an impermeant buffer. Even if the exact nature of the force that contributes to vesicle swelling after a hypertonic shock remains to be studied, the osmotic swelling assay remains a powerful tool to assess membrane permeability.

We thank Dr. Jacques Billette, Department of Physiology, University of Montreal, for his help in dissecting the rabbits.

This work was supported by grants from the Biocontrol Network, the Fonds québécois de la recherche sur la nature et les technologies, the Natural

Sciences and Engineering Research Council of Canada, the Réseau québécois de recherche en phytoprotection, and Valorisation-Recherche Québec.

## REFERENCES

1. Kasai, M., and K. Nunogaki. 1988. Permeability of sarcoplasmic reticulum. *Methods Enzymol.* 157:437–468.
2. Carroll, J., and D. J. Ellar. 1993. An analysis of *Bacillus thuringiensis*  $\delta$ -endotoxin action on insect-midgut-membrane permeability using a light-scattering assay. *Eur. J. Biochem.* 214:771–778.
3. Kasai, M. 1980. Inulin exclusion volume of sarcoplasmic reticulum vesicles under various solvent conditions. *J. Biochem. (Tokyo)*. 88: 1081–1085.
4. Soveral, G., R. I. Macey, and T. F. Moura. 1997. Mechanical properties of brush border membrane vesicles from kidney proximal tubule. *J. Membr. Biol.* 158:209–217.
5. Schnepf, E., N. Crickmore, J. Van Rie, D. Lereclus, J. Baum, J. Feitelson, D. R. Zeigler, and D. H. Dean. 1998. *Bacillus thuringiensis* and its pesticidal crystal proteins. *Microbiol. Mol. Biol. Rev.* 62:775–806.
6. Carroll, J., and D. J. Ellar. 1997. Analysis of the large aqueous pores produced by a *Bacillus thuringiensis* protein insecticide in *Manduca sexta* midgut-brush-border-membrane vesicles. *Eur. J. Biochem.* 245: 797–804.
7. Coux, F., V. Vachon, C. Rang, K. Moozar, L. Masson, M. Royer, M. Bes, S. Rivest, R. Brousseau, J.-L. Schwartz, R. Laprade, and R. Frutos. 2001. Role of interdomain salt bridges in the pore-forming ability of the *Bacillus thuringiensis* toxins Cry1Aa and Cry1Ac. *J. Biol. Chem.* 276:35546–35551.
8. Tran, L. B., V. Vachon, J.-L. Schwartz, and R. Laprade. 2001. Differential effects of pH on the pore-forming properties of *Bacillus thuringiensis* insecticidal crystal toxins. *Appl. Environ. Microbiol.* 67: 4488–4494.
9. Kirouac, M., V. Vachon, J.-F. Noël, F. Girard, J.-L. Schwartz, and R. Laprade. 2002. Amino acid and divalent ion permeability of the pores formed by the *Bacillus thuringiensis* toxins Cry1Aa and Cry1Ac in insect midgut brush border membrane vesicles. *Biochim. Biophys. Acta.* 1561:171–179.
10. Vachon, V., G. Préfontaine, F. Coux, C. Rang, L. Marceau, L. Masson, R. Brousseau, R. Frutos, J.-L. Schwartz, and R. Laprade. 2002. Role of helix 3 in pore formation by the *Bacillus thuringiensis* insecticidal toxin Cry1Aa. *Biochemistry.* 41:6178–6184.
11. Vachon, V., G. Préfontaine, C. Rang, F. Coux, M. Juteau, J.-L. Schwartz, R. Brousseau, R. Frutos, R. Laprade, and L. Masson. 2004. Helix 4 mutants of the *Bacillus thuringiensis* insecticidal toxin Cry1Aa display altered pore-forming abilities. *Appl. Environ. Microbiol.* 70:6123–6130.
12. Peyronnet, O., B. Nieman, F. Génereux, V. Vachon, R. Laprade, and J.-L. Schwartz. 2002. Estimation of the radius of the pores formed by *Bacillus thuringiensis* Cry1C  $\delta$ -endotoxin in planar lipid bilayers. *Biochim. Biophys. Acta.* 1567:113–122.
13. Wolfersberger, M. G., X. J. Chen, and D. H. Dean. 1996. Site-directed mutations in the third domain of the *Bacillus thuringiensis*  $\delta$ -endotoxin Cry1Aa affect its ability to increase the permeability of *Bombyx mori* midgut brush border membrane vesicles. *Appl. Environ. Microbiol.* 62: 279–282.
14. Tigue, N. J., J. Jacoby, and D. J. Ellar. 2001. The  $\alpha$ -helix 4 residue, Asn135, is involved in the oligomerization of Cry1Ac1 and Cry1Ab5 *Bacillus thuringiensis* toxins. *Appl. Environ. Microbiol.* 67:5715–5720.
15. Fortier, M., V. Vachon, M. Kirouac, J.-L. Schwartz, and R. Laprade. 2005. Differential effects of ionic strength, divalent cations and pH on the pore-forming activity of *Bacillus thuringiensis* insecticidal toxins. *J. Membr. Biol.* 208:77–87.
16. Kirouac, M., V. Vachon, D. Quievry, J.-L. Schwartz, and R. Laprade. 2006. Protease inhibitors fail to prevent pore formation by the activated

- Bacillus thuringiensis* toxin CryIAa in insect brush border membrane vesicles. *Appl. Environ. Microbiol.* 72:506–515.
17. Jacobs, M. H. 1952. The measurement of cell permeability with particular reference to the erythrocyte. In *Modern Trends in Physiology and Biochemistry*. E. S. G. Barron, editor. Academic Press, New York. 149–171.
  18. Kedem, O., and A. Katchalsky. 1958. Thermodynamic analysis of the permeability of biological membranes to non-electrolytes. *Biochim. Biophys. Acta.* 27:229–246.
  19. Wolfersberger, M., P. Luethy, A. Maurer, P. Parenti, F. V. Sacchi, B. Giordana, and G. M. Hanozet. 1987. Preparation and partial characterization of amino acid transporting brush border membrane vesicles from the larval midgut of the cabbage butterfly (*Pieris brassicae*). *Comp. Biochem. Physiol.* 86A:301–308.
  20. van de Werve, G. 1989. Liver glucose-6-phosphatase activity is modulated by physiological intracellular  $Ca^{2+}$  concentrations. *J. Biol. Chem.* 264:6033–6036.
  21. Maenz, D. D., C. Chenu, F. Bellemare, and A. Berteloot. 1991. Improved stability of rabbit and rat intestinal brush border membrane vesicles using phospholipase inhibitors. *Biochim. Biophys. Acta.* 1069:250–258.
  22. Maenz, D. D., C. Chenu, S. Breton, and A. Berteloot. 1992. pH-dependent heterogeneity of acidic amino acid transport in rabbit jejunal brush border membrane vesicles. *J. Biol. Chem.* 267:1510–1516.
  23. Masson, L., G. Préfontaine, L. Péloquin, P. C. K. Lau, and R. Brousseau. 1989. Comparative analysis of the individual protoxin components in P1 crystals of *Bacillus thuringiensis* subsp. *kurstaki* isolates NRD-12 and HD-1. *Biochem. J.* 269:507–512.
  24. Masson, L., A. Mazza, L. Gringorten, D. Baines, V. Anelunas, and R. Brousseau. 1994. Specificity domain localization of *Bacillus thuringiensis* insecticidal toxins is highly dependent on the bioassay system. *Mol. Microbiol.* 14:851–860.
  25. van Heeswijk, M. P. E., and C. H. van Os. 1986. Osmotic water permeabilities of brush border and basolateral membrane vesicles from rat renal cortex and small intestine. *J. Membr. Biol.* 92:183–193.
  26. Nobel, P. S. 1969. The Boyle-Van't Hoff relation. *J. Theor. Biol.* 23:375–379.
  27. Mar, T. 1981. Measurement of mitochondrial volume independent of refractive index by light scattering. *J. Biochem. Biophys. Methods.* 4:177–184.
  28. Van der Goot, F., P. Ripoche, and B. Cornan. 1989. Determination of solute reflection coefficients in kidney brush-border membrane vesicles by light scattering: influence of the refractive index. *Biochim. Biophys. Acta.* 979:272–274.
  29. Carpineti, M., F. Ferri, and M. Giglio. 1990. Salt-induced fast aggregation of polystyrene latex. *Phys. Rev. A.* 42:7347–7354.
  30. Rabon, E., N. Takeguchi, and G. Sachs. 1980. Water and salt permeability of gastric vesicles. *J. Membr. Biol.* 53:109–117.
  31. Verkman, A. S., J. A. Dix, and J. L. Seifter. 1985. Water and urea transport in renal microvillus membrane vesicles. *Am. J. Physiol.* 248:F650–F655.
  32. Verkman, A. S., and H. E. Ives. 1986. Water permeability and fluidity of renal basolateral membranes. *Am. J. Physiol.* 250:F633–F643.
  33. Worman, H. J., and M. Field. 1985. Osmotic water permeability of small intestinal brush-border membranes. *J. Membr. Biol.* 87:233–239.
  34. Kometani, T., and M. Kasai. 1978. Ionic permeability of sarcoplasmic reticulum vesicles measured by light scattering method. *J. Membr. Biol.* 41:295–308.
  35. Bravo, A., K. Hendrickx, S. Jansens, and M. Peferoen. 1992. Immunocytochemical analysis of specific binding of *Bacillus thuringiensis* insecticidal crystal proteins to lepidopteran and coleopteran midgut membranes. *J. Invertebr. Pathol.* 60:247–253.
  36. Peyronnet, O., V. Vachon, R. Brousseau, D. Baines, J.-L. Schwartz, and R. Laprade. 1997. Effect of *Bacillus thuringiensis* toxins on the membrane potential of lepidopteran insect midgut cells. *Appl. Environ. Microbiol.* 63:1679–1684.
  37. Johnson, J. A., and T. A. Wilson. 1967. Osmotic volume changes induced by a permeable solute. *J. Theor. Biol.* 17:304–311.
  38. Staverman, A. J. 1951. The theory of measurement of osmotic pressure. *Recl. Trav. Chim. Pays Bas.* 70:344–352.
  39. English, L. H., T. L. Readdy, and A. E. Bastian. 1991. Delta-endotoxin-induced leakage of  $^{86}Rb^{+}$ - $K^{+}$  and  $H_2O$  from phospholipid vesicles is catalyzed by reconstituted midgut membrane. *Insect Biochem.* 21:177–184.
  40. Slaney, A. C., H. L. Robbins, and L. English. 1992. Mode of action of *Bacillus thuringiensis* toxin CryIIIa: an analysis of toxicity in *Leptinotarsa decemlineata* (Say) and *Diabrotica undecimpunctata howardi* Barber. *Insect Biochem. Mol. Biol.* 22:9–18.
  41. Slatin, S. L., C. K. Abrams, and L. English. 1990. Delta-endotoxins form cation-selective channels in planar lipid bilayers. *Biochem. Biophys. Res. Commun.* 169:765–772.
  42. Schwartz, J.-L., L. Gameau, D. Savaria, L. Masson, R. Brousseau, and E. Rousseau. 1993. Lepidopteran-specific crystal toxins from *Bacillus thuringiensis* form cation- and anion-selective channels in planar lipid bilayers. *J. Membr. Biol.* 132:53–62.
  43. Lorence, A., A. Darszon, C. Díaz, A. Liévano, R. Quintero, and A. Bravo. 1995.  $\delta$ -Endotoxins induce cation channels in *Spodoptera frugiperda* brush border membranes in suspension and in planar lipid bilayers. *FEBS Lett.* 360:217–222.
  44. Schwartz, J.-L., Y.-J. Lu, P. Söhnlein, R. Brousseau, R. Laprade, L. Masson, and M. J. Adang. 1997. Ion channels formed in planar lipid bilayers by *Bacillus thuringiensis* toxins in the presence of *Manduca sexta* midgut receptors. *FEBS Lett.* 412:270–276.
  45. Schwartz, J.-L., L. Potvin, X. J. Chen, R. Brousseau, R. Laprade, and D. H. Dean. 1997. Single-site mutations in the conserved alternating-arginine region affect ionic channels formed by CryIAa, a *Bacillus thuringiensis* toxin. *Appl. Environ. Microbiol.* 63:3978–3984.
  46. Peyronnet, O., V. Vachon, J.-L. Schwartz, and R. Laprade. 2001. Ion channels induced in planar lipid bilayers by the *Bacillus thuringiensis* toxin CryIAa in the presence of gypsy moth (*Lymantria dispar*) brush border membrane. *J. Membr. Biol.* 184:45–54.
  47. Meissner, G., and R. Allen. 1981. Evidence for two types of rat liver microsomes with differing permeability to glucose and other small molecules. *J. Biol. Chem.* 256:6413–6422.
  48. Li, W., T. S. Aurora, T. H. Haines, and H. Z. Cummins. 1986. Elasticity of synthetic phospholipid vesicles and mitochondrial particles during osmotic swelling. *Biochemistry.* 25:8220–8229.
  49. Sun, S.-T., A. Milon, T. Tanaka, G. Ourisson, and Y. Nakatani. 1986. Osmotic swelling of unilamellar vesicles by the stopped-flow light scattering method. Elastic properties of vesicles. *Biochim. Biophys. Acta.* 860:525–530.
  50. Ito, T., M. Yamazaki, and S.-I. Ohnishi. 1989. Osmoelastic coupling in biological structures: a comprehensive thermodynamic analysis of the osmotic response of phospholipid vesicles and a reevaluation of the “dehydration force” theory. *Biochemistry.* 28:5626–5630.
  51. Ertel, A., A. G. Marangoni, J. Marsh, F. R. Hallett, and J. M. Wood. 1993. Mechanical properties of vesicles. I. Coordinated analyses of osmotic swelling and lysis. *Biophys. J.* 64:426–434.
  52. Hallett, F. R., J. Marsh, B. G. Nickel, and J. M. Wood. 1993. Mechanical properties of vesicles. II. A model for osmotic swelling and lysis. *Biophys. J.* 64:435–442.